Journal of Solid State Chemistry **146,** 380–386 (1999)
Article ID jssc.1999.8365, available online at http://www.idealibrary.com on IDEAL®

The Crystal Structure of δ-$Na_2Si_2O_5$

V. Kahlenberg, G. Dörsam, M. Wendschuh-Josties, and R. X. Fischer

Fachbereich Geowissenschaften (Kristallographie), Universität Bremen, Klagenfurter Strasse, D-28359 Bremen, Germany

Received January 28, 1999; in revised form April 25, 1999, accepted May 10, 1999

The crystal structure of δ-$Na_2Si_2O_5$ has been solved and refined to an *R* index of 0.053 for 933 independent reflections. The compound is monoclinic with space group $P2_1/n$ ($a = 8.393(2)$ Å, $b = 12.083(3)$ Å, $c = 4.843(1)$ Å, $\beta = 90.37(3)^\circ$, $V = 491.1(1)$ Å^3, $M_r = 182.15$ u, $Z = 4$, $\lambda(MoK\alpha) = 0.71073$ Å, $D_x = 2.46$ g/cm^3, $\mu(MoK\alpha) = 8.3$ cm^{-1}). The crystal showed twinning by pseudo-merohedry according to 2_{100}, a feature which we took account of in the refinements. The compound belongs to the group of single layer silicates. Individual sheets can be described as being built by the condensation of zweier single chains of SiO_4 tetrahedra parallel to the *c*-axis or, alternatively, by condensation of vierer single chains parallel to the *a*-axis. The stacking of the layers parallel to the *b*-axis results in a three-dimensional structure in which the sodium cations reside between the layers for charge compensation. © 1999 Academic Press

INTRODUCTION

Sodium disilicates have been investigated by several authors because of their complex polymorphism (1–4). At least eight different modifications have been reported as a function of temperature, pressure, and synthesis conditions. A summary of selected crystallographic data based on X-ray diffraction experiments for the different $Na_2Si_2O_5$ phases is given in Table 1.

Kanzaki *et al.* (8–9) synthesized another high pressure phase of $Na_2Si_2O_5$ designated ζ-sodium disilicate. Santarsiero *et al.* (10) describe this phase in the trigonal space group $R\bar{3}m$ with $a = 9.898$ Å and $c = 13.0103$ Å and Kanzaki *et al.* (9) give values with $a = 9.896$ Å and $c = 13.005$ Å in hexagonal setting. However, studies by Fleet (11) as well as Fleet and Henderson (7) show that the ζ-phase is most probably a sodium heptasilicate $Na_8Si_7O_{18}$ and, consequently, not a polymorph of sodium disilicate.

A common feature of almost all sodium disilicates is a very short lattice constant of about 4.9 Å. This value corresponds to the translation period along the chain direction in $[Si_2O_6]$ zweier single chains (12), representing a common structural building element in all modifications. The zweier chain period is disturbed in the ε-form, resulting in a vierer single chain with an approximately doubled *c*-lattice constant (in the $P2_1ca$ setting). The crystal structures of Li, Rb, and Cs disilicates are described in (13). Preliminary studies of the δ-phase have been performed by Williamson and Glasser (2). According to their results, the compound is metastable at room temperature. At elevated temperatures the δ-modification transforms irreversibly into the α-phase. The powder pattern was indexed based on an orthorhombic unit cell ($a = 12.07$ Å, $b = 8.37$ Å, $c = 4.84$ Å) (3) and the proposed extinction symbol was *Pn* --. A first structural model for δ-$Na_2Si_2O_5$ has been given by Jacobsen (4) in space group $Pna2_1$. The author showed that the δ-phase has a layer structure with two independent SiO_4 tetrahedra in the asymmetric unit and that the layers are connected by the sodium cations. However, Si–O bond distances vary between 1.46 and 2.09 Å in this model. Tetrahedral angles between 87° and 130° also indicate an extreme distortion. These values are far beyond the spread usually observed in silicate structures and possibly indicate an incorrect choice of space group symmetry. Some deviations between observed peak positions in the X-ray diffraction powder pattern and positions calculated from Jacobsen's structural model also indicate that the symmetry might be lower than orthorhombic (Fig. 1). However, due to the lack of a better model, all deviations so far have been attributed to contributions from an unidentified impurity phase.

The aim of this work is (a) to reexamine the structure of δ-$Na_2Si_2O_5$, (b) to discuss its crystal chemical characteristics, and (c) to compare the structure of the δ-phase with the other modifications.

EXPERIMENTAL

Various amorphous sodium silicates were tested as starting materials for the single crystal growth. Best results were obtained using a water glass solution as already proposed by (1). The solution was applied to the surface of pellets made of fine quartz powder. In contrast to (1) these composites were dried very slowly at a temperature of 75°C for eight weeks, subsequently kept at room temperature for

0022-4596/99 $30.00

TABLE 1
Lattice Parameters and Space Groups for the $Na_2Si_2O_5$ Modifications

Phase	Space group	a (Å)	b (Å)	c (Å)	Monoclinic angle	Reference
α_{III}	$Pcnb$	6.409	15.422	4.896		[5]
α_{II}	mon.	6.64	7.72	4.94	91°	[2]
α_{I}	orthor.	6.64	7.72	4.98		[2]
β	$P112_1/b$	8.133	12.329	4.848	104.2°	[6]
γ	$P12_1/c1$	23.464	7.087	26.120	116.7°	[3]
δ	$P12_1/n1$	8.393	12.083	4.843	90.37°	This work
ε	$P2_1\ ca$	8.356	5.580	9.441		[7]
C	mon.	8.12	23.70	4.85	90°	[2]

Note. Space group settings and unit cell parameters of the β- and ε-disilicate are transformed to the setting of the α_{III}-form.

one week, and then annealed at 700°C for 20 hrs. The product was a white, hard, and porous body. An X-ray powder diffraction pattern showed δ-$Na_2Si_2O_5$ as the main component together with a small amount of α-$Na_2Si_2O_5$. The sample consists of a submicroscopic fine-grained matrix in which several platy crystals of larger size (max. $130 \times 10 \times 140\ \mu m^3$), which could be separated by hand, were embedded.

Experimental details of the data collection for the structure determination are summarized in Table 2. Single crystal intensity measurements were performed using a STOE-imaging plate detector system IPDS at the Department of Chemistry, University of Oldenburg. The data were corrected for Lorentz and polarization effects. No corrections were made for absorption because of the low linear absorption coefficient of 8.3 cm^{-1} for Mo$K\alpha$ radiation.

STRUCTURE SOLUTION, REFINEMENT, AND TWINNING

The analysis of the systematic absences resulted in the assignment of the monoclinic space group $P2_1/n$. A first structural model which conforms to this space group symmetry was found by direct methods, using the program SIR92 (15). Statistical tests on the $|E|$ values indicated the

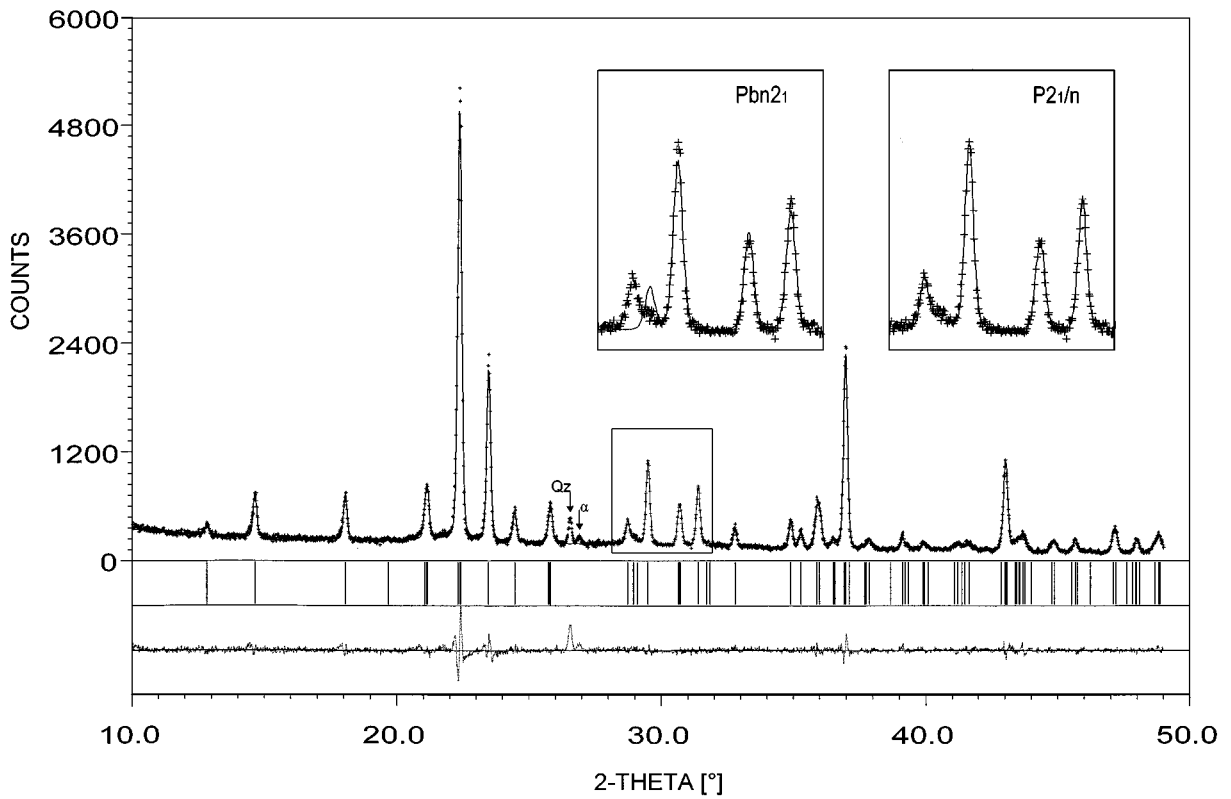

FIG. 1. Observed (crosses) and calculated (solid line) intensities and their difference (dotted line at bottom of figure) of δ-$Na_2Si_2O_5$. The tickmarks indicate peak positions based on the $P2_1/n$ structure model. Small amounts of quartz (Qz) and α-$Na_2Si_2O_5$ (α) are observed. The enlarged region (left frame) shows the most prominent misfit between observed and calculated intensities for the $Pbn2_1$ model (4) in comparison with the $P2_1/n$ model (this study, right frame).The calculated patterns were obtained using the program PC-Rietveld Plus (14).

TABLE 2
Experimental Data of δ-$Na_2Si_2O_5$

(A) Crystal data	
a (Å)	8.393(2)
b (Å)	12.083(3)
c (Å)	4.843(1)
β (°)	90.37(3)
V (Å^3)	491.1(1)
Space group	$P2_1/n$
Z	4
Chemical formula	$Na_2Si_2O_5$
D_{calc} (g cm^{-3})	2.46
μ (cm^{-1})	8.3
(B) Intensity measurements	
Crystal shape	Fragment of a plate
Diffractometer	STOE-IPDS
Monochromator	Graphite
Radiation	Mo$K\alpha$, $\lambda = 0.71073$ Å
Θ-range (°)	3.0–26.1
Reflection range	$\lvert h\rvert \le 10$; $\lvert k\rvert \le 14$; $\lvert l\rvert \le 5$
No. of measured reflections	3285
No. of unique reflections	933
No. of observed reflections ($I > 2\sigma(I)$)	618
(C) Refinement of the structure	
No. of parameters used in the refinement	83
$R1$ ($F_o > 4\sigma(F_o)$)	0.053
w$R2$ ($F_o > 4\sigma(F_o)$)	0.096
Weighting parameter a	0.062
Goodness of fit	0.992
Final $\Delta\rho_{min}$ (e/Å^3)	−0.68
Final $\Delta\rho_{max}$ (e/Å^3)	1.16
$R1 = \sum\lVert F_o\rvert - \lvert F_c\rVert / \sum\lvert F_o\rvert$	w$R2 = (\sum(w(F_o^2 - F_c^2)^2)/\sum(w(F_o^2)^2))$
$w = 1/(\sigma^2(F_o^2) + (aP)^2)$	$P = (2F_c^2 + \max(F_o^2, 0))/3$

TABLE 3
Positional Parameters in Fractional Coordinates and Equivalent Isotropic Displacement Parameters (Å$^2 \times 10^3$)

Atom	x	y	z	U_{eq}[a]
Si(1)	0.9492(2)	0.1974(2)	0.3006(5)	12(1)
Si(2)	0.6764(2)	−0.1793(2)	0.7007(6)	11(1)
Na(1)	0.6303(3)	−0.0025(2)	0.2435(7)	13(1)
Na(2)	0.8804(3)	0.0381(2)	−0.2349(7)	13(1)
O(1)	0.6356(6)	−0.0546(4)	0.7585(12)	10(1)
O(2)	0.8871(6)	0.0762(3)	0.2503(12)	10(1)
O(3)	0.6383(7)	−0.2034(4)	0.3662(11)	18(1)
O(4)	0.5747(6)	−0.2714(4)	0.8654(12)	15(1)
O(5)	0.1396(6)	0.2088(4)	0.2491(11)	14(1)

[a] Defined as one third of the trace of the orthogonalized U_{ij} tensor.

existence of an inversion center. The phase set with the maximum combined figure of merit resulted in an E-map, the most intense peaks of which could be interpreted as the atomic positions of a tetrahedral layer structure. The subsequent refinement calculations were carried out with the SHELXL-93 program (16). Though the model seemed to be reasonable, iterative full matrix least squares calculations based on F^2 using isotropic displacement factors converged to a rather high unweighted $R1$ index of 0.14. The introduction of anisotropic thermal parameters did not significantly improve the refinement. Furthermore, the principal mean square atomic displacement parameters of two oxygen atoms became negative.

Based on these results, a possible twinning of the crystal was taken into consideration in order to explain the difficulties during the refinement. Twinning by pseudo-merohedry is a feature often observed in compounds where the monoclinic angle β is very close to 90°. Assuming the twofold axis 2_{100} as the element of twinning, the fraction of the twin components with the total fraction restrained to 1.0 was introduced into the refinement calculation. The value for $R1$ dropped to 0.068; the value α for twin component 1 refined to 0.271(5). The final refinement using anisotropic diplacement parameters converged at $R1 = 0.053$. The largest shift in the final cycle was < 0.001. The refined atomic coordinates and equivalent isotropic and anisotropic displacement parameters, as well as selected interatomic distances and angles are given in Tables 3–6.

DESCRIPTION OF THE STRUCTURE

The structure of δ-$Na_2Si_2O_5$ consists of a sequence of tetrahedral layers perpendicular to [010] similar to the orthorhombic model proposal in (4). Each layer is composed of six membered rings of SiO_4 tetrahedra in *UDDUDD*—and *DUUDUU*—conformation. Figure 2[1] shows a projection parallel b of one of the two tetrahedral sheets in δ-disilicate compared with the corresponding sheets in α-, β-, and ε-disilicate.

Alternatively, the single layers of δ-$Na_2Si_2O_5$ can be described as being built by condensation of unbranched or loop branched vierer single chains parallel [100] or zweier single chains parallel [001] via common corners (12). A single chain contains Si(1)O_4—as well as Si(2)O_4—tetrahedra. The zweier single chains are similar to those observed in Na_2SiO_3 (17). The equatorial oxygen atoms of the sheets are not strictly coplanar. The layers are corrugated as shown in the projections parallel [001] (Fig. 3a). The bonds between the two symmetrically independent silicon cations and the apical oxygen atoms O(1) and O(2), respectively, are very short (1.57 Å) but are in good agreement with the values for the equivalent nonbridging oxygen atoms in the α- and β-modification. The bond distances between Si(1) and Si(2), respectively, and the three bridging oxygen atoms

[1] For the drawing of the structural details, the computer programs STRUPLO90 (22) and ATOMS (23) were used.

TABLE 4
Anisotropic Displacement Parameters ($Å^2 \times 10^3$) Given as $-2\pi^2[h^2 a^{*2} U_{11} + \cdots + 2hka^*b^*U_{12}]$

Atom	U_{11}	U_{22}	U_{33}	U_{23}	U_{13}	U_{12}
Si(1)	7(1)	7(1)	23(2)	−1(1)	0(1)	2(1)
Si(2)	8(1)	5(1)	21(2)	1(1)	0(1)	0(1)
Na(1)	11(1)	16(1)	12(2)	0(1)	3(2)	0(1)
Na(2)	15(1)	14(1)	10(2)	1(1)	−2(1)	−3(1)
O(1)	13(2)	7(2)	8(3)	−4(2)	2(2)	4(2)
O(2)	18(2)	4(2)	8(3)	0(2)	1(2)	0(2)
O(3)	22(3)	13(3)	18(4)	0(2)	−3(2)	−6(2)
O(4)	18(3)	11(3)	16(4)	−2(2)	−3(2)	−6(2)
O(5)	4(2)	25(3)	12(3)	4(2)	3(2)	5(2)

TABLE 6
Selected Bond Angles (°)

(A) O–T–O angles			
O(2)–Si(1)–O(5)	112.4(3)	O(1)–Si(2)–O(5)	113.4(3)
O(2)–Si(1)–O(3)	117.6(3)	O(1)–Si(2)–O(4)	117.1(3)
O(5)–Si(1)–O(3)	107.7(3)	O(5)–Si(2)–O(4)	106.5(3)
O(2)- Si(1)–O(4)	108.5(3)	O(1)–Si(2)–O(3)	107.4(3)
O(5)–Si(1)–O(4)	104.7(3)	O(5)–Si(2)–O(3)	106.6(3)
O(3)–Si(1)–O(4)	105.0(3)	O(4)–Si(2)–O(3)	105.0(3)
Mean	109.3	Mean	109.4
(B) T–O–T angles			
Si(1)–O(3)–Si(2)	134.0(4)	Si(2)–O(4)–Si(1)	134.3(4)
Si(1)–O(5)–Si(2)	155.0(4)		

of each tetrahedron are considerably longer (average 1.639 and 1.631 Å). While the average values of the O–Si–O angles for the two tetrahedra about Si(1) and Si(2) are very close to the ideal value of 109.47°, the individual O–Si–O angles range from 105° to 118° for the SiO_4 groups. This suggests that the polyhedra are slightly distorted. According to (18) the distortion can be expressed numerically by means of the angle variance σ^2. This parameter has values of 23.8 and 22.6, respectively, for the two $Si(1)O_4$—and $Si(2)O_4$—polyhedra. The angle variance is much higher than the corresponding value for the SiO_4 tetrahedron in α-$Na_2Si_2O_5$ ($\sigma^2 = 9.8$), indicating an increased strain affecting the polyhedra in the δ-phase. The Si(1)–O–Si(2) angles are 134° for the two oxygen atoms O(3) and O(4) within a zweier single chain and 155° about O(5), the anion connecting neighboring chains. The difference between the inter- and intrachain Si–O–Si angles are similar to the corresponding values in α-$Na_2Si_2O_5$ (138° and 160°). The Si–O–Si angles in δ-disilicate agree well with the commonly observed Si–O–Si angle frequency distribution reported by (19) resulting from a statistical analysis of a huge number of different silicate structures. Mean T–O distances of Si(1)–O = 1.623 Å and Si(2)–O = 1.616 Å agree within their standard deviations with the value of 1.617(6) Å given by (20) as a mean distance in phyllosilicates.

TABLE 5
Selected Interatomic Distances (Å)

Si(1)	–O(2)	1.573(5)	Si(2)	–O(1)	1.571(5)
	–O(3)	1.619(6)		–O(5)	1.602(5)
	–O(5)	1.625(5)		–O(4)	1.617(6)
	–O(4)	1.674(6)		–O(3)	1.675(6)
	Mean	1.623		Mean	1.616
Na(1)	–O(1)	2.336(6)	Na(2)	–O(1)	2.340(6)
	–O(2)	2.356(5)		–O(2)	2.392(5)
	–O(1)	2.432(7)		–O(2)	2.395(7)
	–O(3)	2.500(6)		–O(4)	2.417(6)
	–O(1)	2.572(7)		–O(2)	2.536(7)
				–O(5)	2.989(5))
	Mean	2.439		Mean of 5 distances	2.416

Charge balance in the structure is achieved by the incorporation of sodium ions in the channels between tetrahedral layers. The channels along [001] result from folding of the layers. Figure 4 shows a projection of the whole structure along this direction. Within the channels the sodium ions have an irregular coordination with five oxygen neighbors between 2.3 and 2.6 Å. Extending the limit for coordinating anions up to 3.0 Å, Na(2) has an additional ligand at about 2.99 Å. Since typical Na–O bond lengths average about 2.44 Å (21), this latter bond would be very weak.

The crystal structure of δ-$Na_2Si_2O_5$ exhibits close similarities to the α- and β-sodium disilicate structures and the high pressure ε-form. Folded layers of corner connected SiO_4 tetrahedra are the main building units in all four modifications. The six-membered rings (S6R) form honeycomb-like nets in the (010) planes as shown in Fig. 2. Linkage of the fundamental chains parallel [001] yields the straight zweier double chains with all S6R centers aligned on [001]. Condensation of the vierer single chains along [100] results in a zigzag pattern of the S6R. In β- and ε-disilicate the S6Rs are elliptically distorted with alternating orientations in the adjacent double chains along [001]. The cell constant c is approximately doubled in the ε-form due to the doubling of the chain periodicity in [001]. Its short translation period in [010] is achieved by the strict parallelism of the layers (Fig. 3d). In the α-, β-, and δ-modifications, neighboring layers are twisted by 180° about the 2_1-axes which are parallel b in the α- and δ-disilicate and parallel c in the β-form.

The relative orientation of the tetrahedra as well as the degree of corrugation in the layers differ considerably, however, between the varous modifications. The comparison between the projections of the single layers parallel to the chain directions (Fig. 3a–3c) reveals: (a) within a single sheet in δ- and α-$Na_2Si_2O_5$ all tetrahedra point either toward the

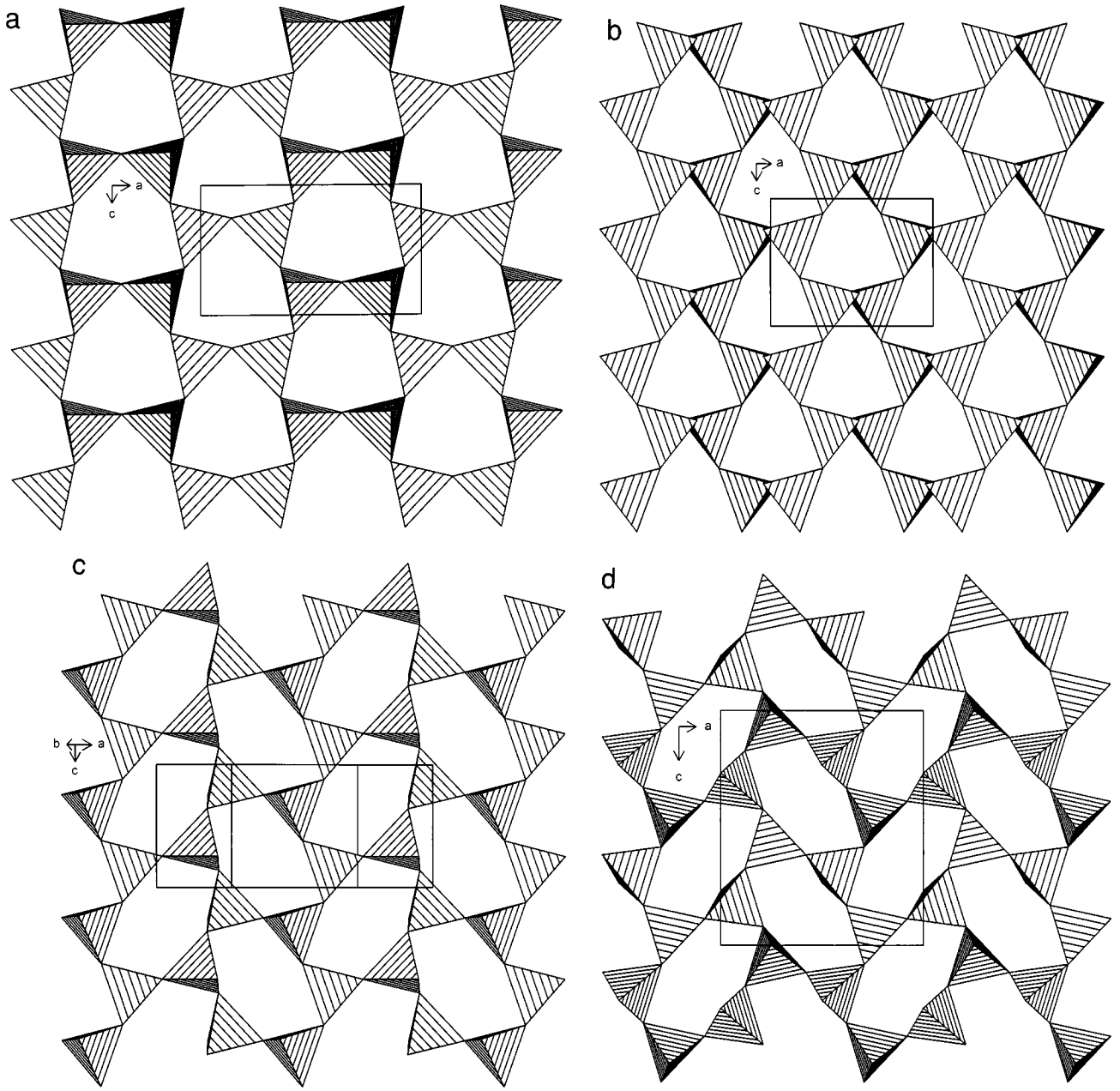

FIG. 2. Single tetrahedral layers of the SiO_4 tetrahedra in sodium disilicates. (a) δ-, (b) α-, (c) β-, and (d) ε- $Na_2Si_2O_5$.

observer or in the opposite direction. In the β-phase the tetrahedra of neighboring chains in a layer show a reversed orientation; (b) the crimping of the layers in α-disilicate is much more pronounced than in the other two modifications. As a result, the lattice constant of α-disilicate parallel to the amplitude of the folding (perpendicular to the layers) increases by about 27% relative to the δ-phase, whereas the lattice constant in the wavelength direction decreases by about the same factor. The degree of folding in the β-phase is comparable to that observed in δ-$Na_2Si_2O_5$. The high pressure ε-form does not show this type of folding (Fig. 3d). It consists of approximately straight chains along [100] where all tetrahedra point up toward [010] in one chain (densely hatched) and point down toward [0 −10] in the neighboing chains (less dense) in alternating sequence.

The occurrence of two crystallographically different Si sites contradicts observations from ^{29}Si MAS-NMR analyses (24). These studies indicated that the δ-modification consists of identical SiO_4 tetrahedra. Since there is no doubt about the corrrect assignment of the Si atoms in the single

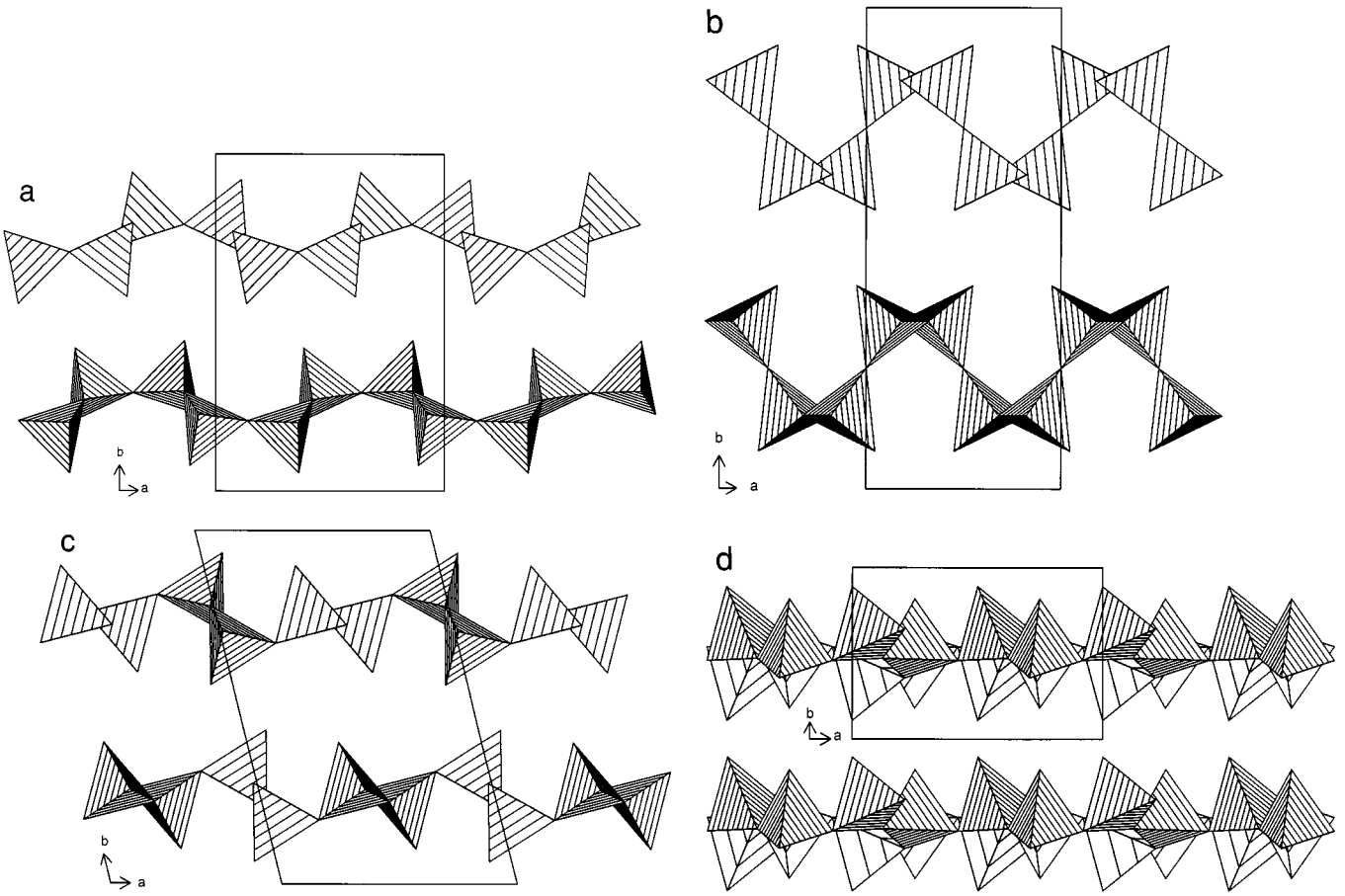

FIG. 3. Side view parallel c of the layers shown in Fig. 2. (a) δ-, (b) α- (c) β-, and (d) ε- $Na_2Si_2O_5$.

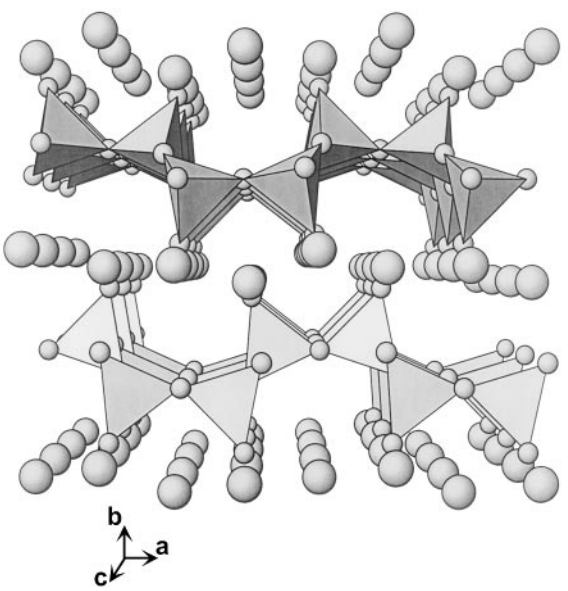

FIG 4. Perspective view of the whole crystal structure of δ-$Na_2Si_2O_5$ parallel to [001]. The large spheres in the interstitial sites represent Na atoms.

crystal structure determination, the NMR signal could be explained by superposition of the two Si atoms with similar environments. This is, e.g., expressed by the similarities between the two crystallographically nonequivalent T–O–T angles of 134° which are identical within their standard deviations. However, it should be pointed out that the mean Si–O distances of 1.623 and 1.616 Å for Si(1)–O and Si(2)–O, respectively, are in excellent agreement with the corresponding values of 1.622 and 1.620 Å proposed from the NMR studies. Further, the single crystal analysis also confirmed that the two Na atoms are coordinated by five and six oxygen atoms, respectively, as suggested already in the NMR study.

The δ-$Na_2Si_2O_5$ exhibits the largest S6R openings of all four modifications and assumes a more circular shape. This might explain its superior ion exchange properties relative to the other modifications.

ACKNOWLEDGMENTS

We thank G. Schimmel, H. Bauer, and J. Holz of Clariant GmbH (Knapsack) for support and helpful discussions and C. Devey (Univ. of

Bremen) for his comments. The single crystal data collection of W. Saak (University of Oldenburg) and the help of A. Piotrowski (University of Bremen) are gratefully acknowledged.

REFERENCES

1. A. Willgallis and K. J. Range, *Glastechnische Berichte* **37,** 194 (1963).
2. J. Williamson and F. P. Glasser, *Phys. Chem. Glasses* **7,** 127 (1966).
3. W. Hoffmann and H. J. Scheel, *Z. Kristallogr.* **129,** 396 (1969).
4. H. Jacobsen, "Neue Untersuchungen an Natriumdisilikat ($Na_2Si_2O_5$)," Master thesis, University of Hannover, 1991.
5. A. K. Pant and D. W. J. Cruickshank, *Acta Crystallogr*., *B* **24,** 13 (1968).
6. A. K. Pant, *Acta Crystallogr*., *B* **24,** 1077 (1968).
7. M. E. Fleet and G.S. Henderson, *J. Solid State Chem.* **119,** 400 (1995).
8. M. Kanzaki, X. Xue, and J. F. Stebbins, *EOS Trans. Am. Geophys. Union* **70,** 1418 (1989).
9. M. Kanzaki, X. Xue, and J. F. Stebbins, *Phys. Earth Planet Int*. **107,** 9 (1998).
10. B. D. Santarsiero, X. Xue, and M. Kanzaki, *Trans. Am. Crystallogr. Assoc.* **27,** 279 (1991).
11. M. E. Fleet, *Am. Mineral*. **83,** 618 (1998).
12. F. Liebau, "Structural Chemistry of Silicates," Springer-Verlag, Berlin 1985.
13. B. H. W. S. de Jong, P. G. G. Slaats, H. T. J. Supèr, N. Veldman, and A. L. Spek, *J. Non-Cryst. Solids* **176,** 164 (1994).
14. R. X. Fischer, C. L. Lengauer, E. Tillmanns, R. J. Ensink, C. A. Reiss, and E. J. Fantner, *Mater. Sci. Forum* **133–136,** 287 (1993).
15. A. Altomare, G. Cascarano, C. Giacovazzo, A. Guagliardi, M. C. Burla, G. Polidori, and M. Camalli, *J. Appl. Cryst*. **27,** 435 (1992).
16. G. M. Sheldrick, SHELXL-93. Program for the refinement of crystal structures University of Göttingen, Germany, 1993.
17. W. S. McDonald and D. W. J. Cruickshank, *Acta Crystallogr*., **22,** 37 (1967).
18. K. Robinson, G. V. Gibbs, and P. H. Ribbe, *Science* **171,** 560 (1971).
19. W. Baur, *Acta Crystallogr.*, *B* **36,** 2198 (1980)
20. W. Baur, *Acta Crystallogr*., *B* **34,** 1751 (1978)
21. A. J. C. Wilson, Ed., "International Tables for Crystallography, Volume C, Mathematical, Physical and Chemical Tables," Kluwer, Dordrecht, 1995.
22. R. X. Fischer, A. LeLirzin, D. Kassner, and B. Rüdinger, *Z. Kristallogr. Suppl.* **3,** 75 (1991)
23. E. Dowty, ATOMS-Shape Software, 1997.
24. D. Heidemann, C. Hubert, W. Schwieger, P. Grabner, K.-H. Bergk, and P. Sarv, *Z. Anorg. Allg. Chem.* **617,** 169 (1992).